Proceedings of the 2nd Biennial IEEE/RAS-EMBS International Conference on Biomedical Robotics and Biomechatronics Scottsdale, AZ, USA, October 19-22, 2008

Biomimetic Orthosis for the Neurorehabilitation of the Elbow and Shoulder (BONES)

J. Klein, *Student Member, IEEE,* S.J. Spencer, *Student Member, IEEE* , J. Allington, K. Minakata, E.T. Wolbrecht, R. Smith, J. E. Bobrow, *Member, IEEE*, and D. J. Reinkensmeyer, *Member, IEEE*

***Abstract*—This paper presents a novel design for a 4 degree of freedom pneumatically-actuated upper-limb rehabilitation device. BONES is based on a parallel mechanism that actuates the upper arm by means of two passive, sliding rods pivoting with respect to a fixed structural frame. Four, mechanically-grounded pneumatic actuators are placed behind the main structural frame to control shoulder motion via the sliding rods, and a fifth cylinder is located on the structure to control elbow flexion/extension. The device accommodates a wide range of motion of the human arm, while also achieving low inertia and direct-drive force generation capability at the shoulder. A key accomplishment of this design is the ability to generate arm internal/external rotation without any circular bearing element such as a ring, a design feature inspired by the biomechanics of the human forearm. The paper describes the rationale for this device and its main design aspects including its kinematics, range of motion, and force generation capability.**

***Index Terms*—arm exoskeleton, rehabilitation, stroke**

I. Introduction

LAST year there were about 780,000 stroke episodes in the U.S., a number that has increased yearly over the past decade due to an increase in the mean age of the U.S. population. From 1994 to 2004, the stroke survival rate also improved 24.2 percent. The estimated direct and indirect cost of stroke for 2008 is $65.5 billion. [1].

The result of more people having and surviving strokes is an increased need for rehabilitation services. Stroke patients with hemiparesis usually suffer difficulty with daily activities such as reaching, grasping, or walking [2]. Stroke survivors undergo rehabilitation therapy to improve movement ability, and it has been demonstrated that rehabilitation progress depends on the training intensity [3]. However, patients are receiving less therapy now than 20 years ago due to economic constraints on the U.S. health care system [4].

In recent years there has been increasing interest in using robotic devices to help automate rehabilitation therapy for stroke patients [5]. Such devices may ultimately allow patients improved access to repetitive aspects of movement training at a reduced cost. Many upper limb robotic devices have been developed [e.g. 6-14].

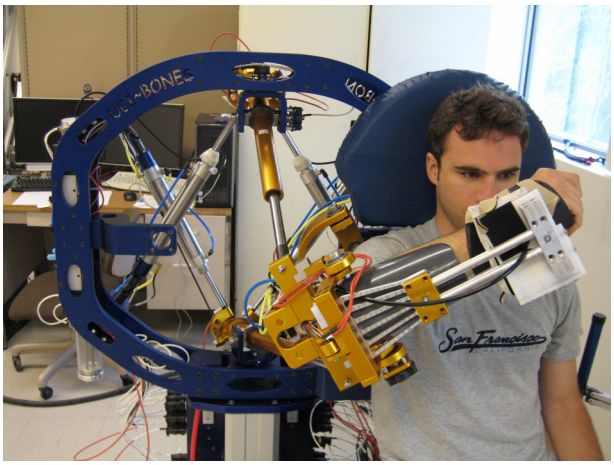

Fig. 1. Healthy subject on the first prototype of BONES.

These devices have shown initially positive clinical results: patients who receive robotic therapy in the chronic or acute stages following stroke significantly improve their movement ability [3]. However, movement ability gains due to robotic therapy are small, and typically do not transfer to activities of daily living [3]. A key question for the field is therefore "How can robotic therapy be optimized to improve these initially positive clinical results?"

Strategies for optimizing robotic therapy include designing improved exercise protocols, developing more sophisticated control algorithms, and improving the mechanical design of the robots. This paper focuses on the last strategy: improved mechanical design. Most previous robotic therapy devices have used a reduced number of DOF compared to the human arm [15-19]. Therefore, the movements trained with these devices are not fully naturalistic. Motor learning research suggests that motor learning is task specific [20]: i.e. that transfer of skill to other movements following training of one movement is limited. Therefore, one way to improve robotic therapy may be to develop devices that allow patients to practice movements that are kinematically more similar to activities of daily living.

Naturalistic arm movements can be accommodated with 5 or 6 DOF industrial robots [21, 22], but these robots do not

Manuscript received August 31, 2008. This work was supported in part by NIH N01-HD-3-3352 and NCRR M01RR00827.

J. Klein, S.J. Spencer, J. Allington, K. Minakata, R. Smith, J. E. Bobrow, and D. J. Reinkensmeyer are with the University of California Irvine, Irvine, CA 92697 USA (phone: 949-824-8057; fax: 949-824-8585; e-mail: juliusk@uci.edu).

E.T. Wolbrecht is with the Mechanical Engineering Department, University of Idaho, Moscow ID 83844 USA.

match the workspace of the human arm, limiting functional movements and raising safety issues. Several groups are also developing robotic exoskeletons to meet the goal of more naturalistic arm movements [6, 23-26]. These devices typically use a serial-chain design in which actuators are mounted on progressively more distal serially-connected links of the robot. A common strategy is to achieve upper arm internal/external rotation using serially-mounted rings bearings [25, 27-31] with an actuator mounted directly on the ring.

Reducing weight and inertia with this serial strategy while still achieving good force control typically necessitates use of small, highly geared actuators and force feedback, a strategy that has been implemented with success [6, 31]. However, this strategy has the limitations that the endpoint impedance of the robot at high frequencies tends to infinity, and the weight and inertia of the robot are necessarily determined by the actuator selection.

An alternate strategy to achieving a lightweight robot with good force control is to use a parallel mechanism with mechanically grounded actuators. For example, the MIT-MANUS robot uses two mechanically grounded actuators at the shoulder to control planar motion of the robot end effector. This strategy has the advantage that it allows large, direct-drive actuators to be used to generate force, since the weight of the actuators themselves need not be moved. Extending such a design to more than 2 DOF is difficult though because of the need for complex mechanisms [32].

We previously developed a parallel robot (Pneu-WREX) that allows 3 DOF movement of the arm using mechanically grounded pneumatic actuators [9, 34]. Pneu-WREX is currently being evaluated in a clinical trial of robotic therapy. Pneu-WREX does not allow shoulder-external rotation, as it was based on a passive weight supporting orthosis design [36] that did not include this degree of freedom in order to improve the weight balance. However, feedback from therapists suggests that this degree of freedom is perceived as very important for stroke rehabilitation.

This paper presents the design of a new robot (BONES) that uses a simple parallel mechanism with mechanically grounded actuators to achieve 3 DOF shoulder movement, including shoulder internal/external rotation [37]. The robot incorporates a serially-placed actuator for elbow flexion/extension, but uses a pneumatic actuator for this DOF to achieve large force output with light weight (Fig. 1).

II. Design Description

The inspiration for the design used in BONES (Fig. 2) was the human forearm. In the human forearm, the ulna and the radius bones prescribe a unique and complex motion in order to supinate/pronate the wrist [38]. We used a simplified model of the human internal forearm mechanism consisting of an external pair of actuators that wrap around the upper arm, hence the word 'biomimetic'.

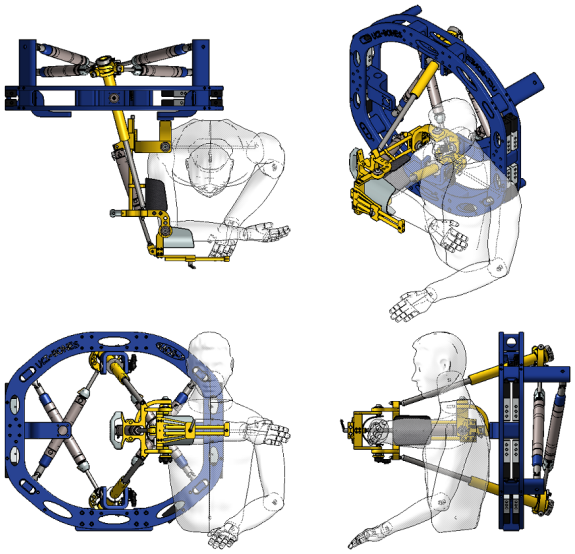

Fig. 2. Several rendered views of the main components of BONES.

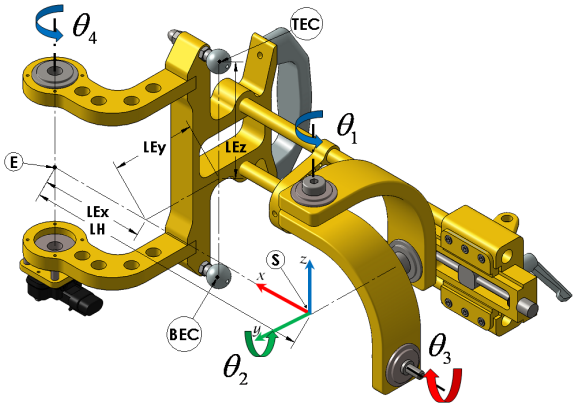

Fig. 3. CAD model of the upper arm exoskeleton. S represents the location the subject's shoulder. E represents the location the center of the subject's elbow. TEC is one of the two points through which the upper arm exoskeleton is actuated. BEC is the second point through which the actuation takes place.

A. Mechanism Design Details

The upper arm exoskeleton (Fig. 3) mimics the upper arm motion as a spherical joint rotating about the shoulder (Fig. 5, point *S*). The flexion/extension rotation of the subject's Humerus is aligned along the *x*-axis (*S* to *E*). The elbow joint coincides with the upper arm's *x*-axis at point *E*. The upper arm lengths (*LH*) can be adjusted in order to accommodate a wide range of subjects.

The arm is actuated at the elbow by means of two rods that can passively slide. One rod pivots with respect to static point *YT* (at the center of rotation of the top yoke, which is attached to the actuators) and is attached to the arm exoskeleton at point *TEC*. Note that *TEC* is not aligned with the elbow rotation axis, yet the point is close to the location of the subject's elbow theoretical center. For simplicity we named this point Top Elbow Connection (*TEC*). Similarly, the other rod pivots at *YB* (bottom yoke center of rotation) and is attached to the arm at *BEC* (bottom elbow connection point).

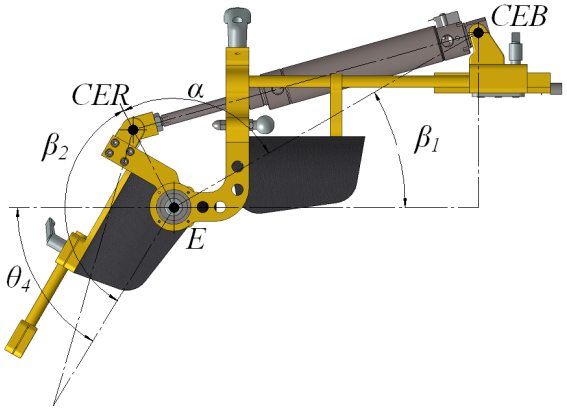

Fig. 4. Elbow flexion/extension mechanism.

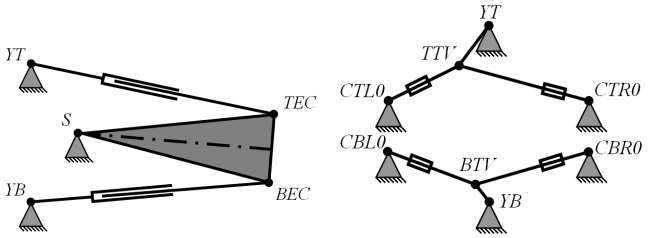

Fig. 5. (left) Elbow motion diagram. (right) Rear 'Diamond Structure' actuation diagram.

Both rods extend past *YT* and *YB*, respectively, towards the back of the robot's frame. The rear end of each these rods is actuated by two pneumatic cylinders using the scheme depicted in Fig. 6 (we refer to this configuration as the 'Diamond Structure'). The Diamond Structure includes two geometric tetrahedrons. The static base of the first tetrahedron is defined by *CTL0*, *YT* and *CTR0*. The vertex of the first tetrahedron is *TTV* ('Top Tetrahedron Vertex'). Similarly, the second tetrahedron has a base defined by *CBL0*, *CBR0* and *YB*. Its corresponding vertex is *BTV* (Bottom Tetrahedron Vertex). The upper rod contains the points *TTV* (rear end), *YT* (yoke pivot point) and *TEC* (elbow actuation point). Similarly, the lower rod aligns *BTV*, *YB* and *BEC*.

The distances from *BTV* to *YB* and from *TTV* to *YT* are fixed, but the distance from *YT* to *TEC* and from *YB* to *BEC* varies passively depending on the position of the exoskeleton. If points *TTV* and *BTV* are moved to the right, the arm moves to the left. When points *TTV* and *BTV* are moved downward, the arm moves up. If *TTV* and *BTV* are displaced in opposing directions, the elbow rotates about the *x*-axis (internal/external rotation). In Fig. 6, several configurations for the rear diamond are shown.

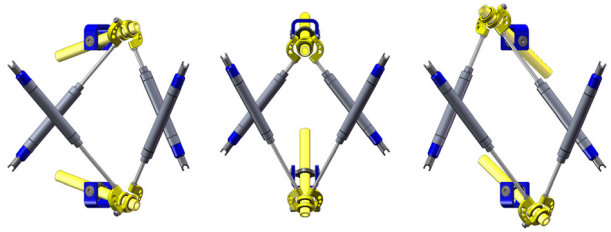

Fig. 6. Rear view of the 'Diamond Structure' for the elbow.

In order for the pairs of cylinders to actuate the tetrahedron vertices, we designed a mechanism (Fig. 7) that mimics a spherical joint by intersecting the two cylinder axis and the rod axis at *TTV* (or *BTV*).

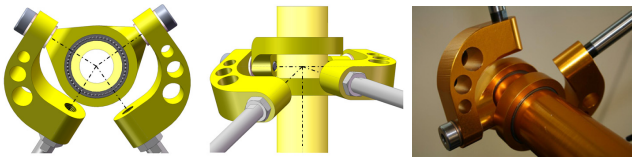

Fig. 7. (left and center) CAD model of spherical joint mechanism. (right) Actual part used in the first BONES prototype.

B. Range of Motion

The range of motion (ROM), or workspace, achieved by BONES is summarized in Table I. Note that we define home position to be $[\theta_1, \theta_2, \theta_3, \theta_4] = [0, 0, 0, 0]$, according to the angles described in Fig. 3. In this position, the upper arm is horizontal, aligning the elbow and the shoulder at the same elevation, and the forearm fully extended. The ROM is close to human ROM, except at the elbow, where we limit elbow flexion to prevent the robot from contacting the subject's torso.

TABLE I
RANGE OF MOTION

	BONES (Min.) [degrees]	BONES (Max) [degrees]	BONES Range of Motion [degrees]	ADL Range of Motion [degrees]
θ_1	-45	60	105	110
θ_2	-35	45	80	100
θ_3	-40	60	100	135
θ_4	14	84	70	150

Angles are measured with respect to the home position and shown in Fig. 3. The desired angles are obtained from [39].

C. Hardware, actuators, and sensors

We incorporated pneumatic cylinder actuators and sensors into BONES, as described next. It would also be possible to use the same mechanism design with other types of actuators, including linear or rotary electric motors. Direct drive rotary actuators could be mounted at the yokes, for example.

The main structural frame (Fig. 2) consists of two oval-shaped aluminum plates (76.2cm x 86.3cm) separated by a 6.4cm gap. The gap between the two plates is used to enclose 10 Festo MPYE-5-1/8-LF-010-B proportional directional control valves. This gap is also used to route the sensor wiring, power supply and air supply, in order to provide protection and making the overall design more aesthetically pleasing.

Previous work in our research group [35] revealed the importance of having the pneumatic valves and the pressure sensors as close to the cylinder as possible in order to minimize pressure loss, latency due to pressure wave dynamics, and obtain more accurate cylinder pressure measurements. In order to locate the pressure sensors close to the cylinder chambers, we customized both ends of the

double actuated Bimba cylinders as a means to provide an attachment port for a Honeywell ASCX100AN pressure sensor (Fig. 8). We machined a flat surface on both ends of the cylinder and drilled a precision hole into the chamber in order to allow the pressure sensing port to become embedded directly inside the cylinder chamber. This solution enables a clean and direct pressure reading while minimizing the required plumbing parts. During the machining process, the chamber was pressurized at 0.68MPa (100PSI) so that any possible contaminating lubricant fluid or chip was blown away from the cylinder chamber.

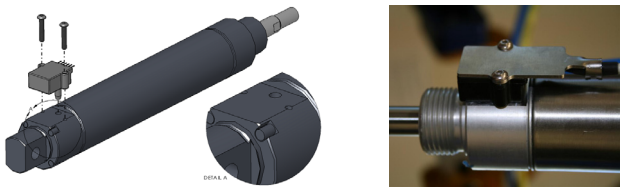

Fig. 8. (left) CAD exploded view of the assembly of the post-processed cylinder and the pressure sensor. (right) Actual view of the finished assembly.

Five PFC-XLBP Bimba low-friction, position feedback cylinders are used to actuate BONES. Although the mechanism presents 4 DOF, we use one extra cylinder in the rear Diamond Structure (Fig. 5) in order to achieve higher forces, higher stiffness control, and add redundancy of measurements for safety purposes.

BEI Duncan 9855R5K low profile potentiometers are located at the elbow joint and at each of the two revolute axes of the yokes (located at point *YT* and *BT* in Fig. 5).

The bearing surfaces for all revolute joints (elbow joint, shoulder spherical link and upper and lower yokes) use flanged tapered A4138B Timken bearings. We use tapered bearings to minimize backlash while maintaining a smooth, low friction rolling joint. The overall assembly presents very low backlash and friction simultaneously.

The device can be adapted to the anthropometry of a wide range of stroke patients. The arm length (from S to E) can be adjusted to accommodate 27.9 cm (11 in) to 44.4 cm (17.5 in) long arms. Furthermore, in order to align the subject's shoulder to the exoskeleton's *S* point, the mechanism is provided with an electrically adjustable 30.5 cm (12 in) stroke pedestal and a motorized chair base capable of fine tuning the subject's elevation by 10.1 cm (4 in) in the vertical direction, and 5.1 cm (2 in) in the lateral direction. BONES can also be easily reconfigured from right to left arm configuration and vice versa.

D. Kinematics

In this section, we present the inverse kinematics for the mechanism, which allow us to solve for the cylinder coordinates to produce a desired joint motion of the human arm.

Although there exist recommendations from the International Society of Biomechanics on how to define a joint coordinate system for the upper limb [40, 41], for simplicity we used the homogenous transformations similar to the Euler angles proposed in [41]. While the rotation sequence *XZX* is the common Euler angle formulation found in [43], we used the sequence *ZYX* which has singularities when *Y* is ±90 degrees. In our case, this singularity is not in the range of motion of the robot. To solve the kinematics of the robot, we defined the following coordinate systems, angles and transformations:

$\{F_0\}$ is the reference frame with origin at *S*, and x_0-axis aligned to the line defined by *S* and *E*. The z_0-axis, as shown in Fig. 3, is vertical pointing upward, orthogonal to the x_0-axis. Accordingly, the y_0-axis completes $\{F_0\}$ as an orthogonal right-handed coordinate system. The angle θ_1 represents a rotation about the z_0-axis. The coordinate system $\{F_1\}$ is the result of rotating $\{F_0\}$ with respect to z_0. Furthermore, θ_2 represents a rotation about the y_1-axis. $\{F_2\}$ is the result of rotating $\{F_1\}$ about y_1. In addition, θ_3 represents a rotation about the x_3-axis.The explicit functions of *TEC* and *BEC* (both defined in the previous section) in the coordinate system $\{F_0\}$ are

$$TEC = R_z(\theta_1)\cdot R_y(-\theta_2)\cdot R_x(\theta_3)\cdot TEC_0 \qquad (1)$$

and

$$BEC = R_z(\theta_1)\cdot R_y(-\theta_2)\cdot R_x(\theta_3)\cdot BEC_0\,. \qquad (2)$$

Note that, according to the dimensional parameters described in Fig. 3, the homogeneous coordinates of TEC_0 and BEC_0 are

$$TEC_0 = \begin{bmatrix} LEH - LE_z \\ -LE_y \\ LE_z \\ 1 \end{bmatrix} \quad \text{and} \quad BEC_0 = \begin{bmatrix} LEH - LE_z \\ -LE_y \\ -LE_z \\ 1 \end{bmatrix}.$$

Within the workspace of the human arm, for any given combination of *roll*, *pitch* and *yaw* transformations the location of *TEC* and *BEC* is unique.

Once the location of *TEC* and *BEC* is defined, we continue the kinematic analysis at the Diamond Structure. We express the location of the rear end of the upper and bottom rods in terms of the elbow connection points as

$$TTV = -\frac{TEC - YT}{|TEC - YT|}|TTV - YT| + YT \qquad (3)$$

and

$$BTV = -\frac{BEC - YB}{|BEC - YB|}|BTV - YB| + YB\,. \qquad (4)$$

Having determined the location of *TTV* and *BTV*, we

define the cylinder coordinates for the four cylinders in the Diamond Structure (Fig. 5) and the elbow cylinder (Fig. 4) as

$$q = \begin{bmatrix} |TTV - CTL0| \\ |TTV - CTR0| \\ |BTV - CBL0| \\ |BTV - CBR0| \\ |CER - CEB| \end{bmatrix}. \quad (5)$$

The elbow joint coordinate can be determined independently from the previous calculations due to the fact that the elbow is decoupled from the Diamond Structure actuators. We define the edges of the triangle defined by the points *CEB*, *E*, *CER* (Fig. 4) as follows:

$$a = |CER - CEB| \quad (6)$$

$$b = |E - CER| \quad (7)$$

$$c = |E - CEB| \quad (8)$$

Using law of cosines we obtain the following relation,

$$a^2 = b^2 + c^2 - 2bc\cos(\alpha). \quad (9)$$

From (5) and (6) we can establish the relation $a = q_5$. According to the notation used in Fig. 4, it holds that

$$\theta_4 + \pi = \beta_1 + \alpha + \beta_2. \quad (10)$$

Finally, using (9) and (10), the fifth cylinder coordinate as a function of the elbow angle, θ_4, is determined by

$$q_5 = \sqrt{b^2 + c^2 - 2bc\cos(\theta_4 + \pi - \beta_1 - \beta_2)}. \quad (11)$$

where β_1, β_2 are constant.

III. FORCE GENERATION

A. Relating Cylinder Forces, Joint Torques, and Endpoint Forces

If the set of desired arm angular velocities are known, the necessary cylinder linear velocities are given by:

$$\dot{q} = \frac{dq}{dt} = \frac{\partial f}{\partial \theta}\dot{\theta} = J_c(\theta)\dot{\theta}, \quad (12)$$

where $q(t) \in \Re^5$, $\theta(t) \in \Re^4$, $f(\theta): \Re^4 \to \Re^5$, and thus $J_c \in \Re^{5\times 4}$. The transpose of the Jacobian relates the torques applied to the arm, τ, to the forces by the actuators, F_c:

$$\tau = J_c^{\mathsf{T}}(\theta) F_c. \quad (13)$$

We use two different Jacobians for BONES. One relates cylinder velocities to the robot joint velocities. The other relates robot joint velocities to wrist/forearm velocities in a world-centered frame. The first Jacobian is important for relating the actuators forces to the joint torques. The second Jacobian is important for determining the forces that the robot applies to the subject in endpoint coordinates.

The location of the wrist can be described by the kinematic chain formed from the 4 joint angles in the shoulder and elbow, similarly to how *TEC* and *BEC* were defined but with an additional transformation for the elbow. Using this transformation, three DOF of the wrist can be easily defined as the resulting position of the wrist. A coordinate for the last DOF of the wrist needs to be defined from the rotation matrix of the transformation. Using the swivel angle [44] as this final coordinate, a coordinate transformation from shoulder and elbow angles to wrist position and arm swivel can be defined as

$$q_w = g(\theta). \quad (14)$$

Taking the derivative of this equation with respect to time gives us the arm Jacobian in

$$\dot{q}_w = \frac{dq_w}{dt} = \frac{\partial g}{\partial \theta}\dot{\theta} = J_a(\theta)\dot{\theta}. \quad (15)$$

The cylinder Jacobian is found using (12) on (1)-(5). The Jacobian equations are too long to be provided in this paper.

B. Passive Gravity Support

Elastic elements located in parallel with cylinders 1, 2 and 3 provide weight support for the exoskeleton. In case of emergency or power outage, the exoskeleton returns to the home position, so the subject's arm does not fall. The elements also bias the force operating range of the actuators so that they have a greater, bi-directional range.

The adjustment of these elastic elements was determined from (13) at the home position. If we substitute pneumatic cylinders with spring-like elements, then we can use (13) to determine the forces required by these springs in order to achieve a desired torque to the arm. Note that we are using 3 spring-like elements, and not 4. This allows us to use a 3x3 submatrix of J_c, corresponding to a 3x1 F_c vector associated to the springs. This submatrix is invertable and allows us to calculate the required forces to balance the exoskeleton at the home position using

$$\left(J_c^{\mathsf{T}}(\theta)\right)^{-1}\tau = F. \quad (19)$$

C. Joint Torque Range

We have attached 3.81cm (1.5in) diameter pneumatic cylinders to the device, and will operate them at 90 PSI. With these numbers, the peak force generating capability of BONES is summarized in Table II.

TABLE II
TORQUES APPLIED TO THE ARM

	BONES [Nm]	Impaired Arm [Nm]	Unimpaired Arm [Nm]	ADL [Nm]
τ_1	75	27.18	53.90	8
τ_2	108	41.20	53.53	10
τ_3	42	19.08	35.55	1
τ_4	68	38.73	80.93	3.5

Impaired arm data from [45]. ADL extracted from [39].

For BONES, we are targeting patients with severe to moderate arm impairment (Upper Extremity Fugl-Meyer Score less than 35 out of 66 max [46]). For this level of impairment, the device's maximum torque is larger than the impaired arm's maximum torques. If higher force levels are required, larger diameter cylinders can replace the existing ones, or supply pressure can also be increased.

TABLE III
INERTIA OF THE EXOSKELETON

	axis	BONES [g·cm^2 X10^3]	Human [g·cm^2 X10^3]
Upper arm	X	165	39.8
	Y	696	204.4
	Z	740	190.5
Forearm	X	53	18.8
	Y	281	124.8
	Z	414	122.4

Human data values have been extracted from [47].

The upper arm exoskeleton weighs 3438g (including the elbow actuator). The forearm exoskeleton module weighs 921g for a total arm weight of 4359g. An average (across sexes) human upper arm weighs approximately 2500g, and a human forearm, 1720g, for a total of 4220g [47]. Thus, the mass of the exoskeletal parts that the subject has to move is comparable to the mass of a human arm. This relatively lightweight exoskeleton is made possible by the use of the parallel mechanism and mechanical grounded actuators. Indeed, the total weight of the robot, including the mechanically grounded actuators, is 18.5kg. Mass could be further reduced in the next version of BONES by reducing part size.

IV. CONCLUSION

This paper presented the design and kinematic analysis of BONES, a novel robot that allows naturalistic motion of the human arm using mechanically grounded, direct drive actuators at the shoulder. Direct drive actuation is achieved with a relatively simple mechanism inspired by the human forearm. The range of motion, inertia, and force generating capacity of the mechanism are well matched to the human arm. In the clinic, we plan to use BONES to assist, resist, and perturb naturalistic arm movements for the purpose of re-training movement ability after stroke. Development of BONES will allow us to rigorously test whether functional transfer of robotic therapy is improved by practicing more naturalistic movements, and will allow implementation of a wide variety of force assistance algorithms.

REFERENCES

[1] Heart Disease and Stroke Statistics - 2008 Update, American Heart Association

[2] National Institute of Neurological Disorders and Stroke http://www.ninds.nih.gov/disorders/stroke/poststrokerehab.htm

[3] G. Kwakkel, R. van Peppen, R. C. Wagenaar, S. Wood Dauphinee, C. Richards, A. Ashburn, K. Miller, N. Lincoln, C. Partridge, I. Wellwood and P. Langhorne, "Effects of Augmented Exercise Therapy Time After Stroke: A Meta-Analysis," *Stroke*, vol. 35, pp. 2529-2539, November 1. 2004.

[4] S. M. Schmidt, L. Guo and S. J. Scheer, "Changes in the status of hospitalized stroke patients since inception of the prospective payment system in 1983," *Archives of Physical Medicine and Rehabilitation*, vol. 83, pp. 894-898, 7. 2002.

[5] B. Brewer, S. K. McDowell and L. C. Worther-Chaudhari, "Poststroke Upper Extremity Rehabilitation: A Review of Robotic Systems and Clinical Results," *Topics in Stroke Rehabilitation*, vol. 14(6), pp. 22-44, Nov-Dec. 2007.

[6] T. Nef, M. Mihelj, G. Kiefer, C. Perndl, R. Muller and R. Riener, "ARMin - exoskeleton for arm therapy in stroke patients," in *Rehabilitation Robotics, 2007. ICORR 2007. IEEE 10th International Conference on,* 2007, pp. 68-74.

[7] A. Sledd and M. K. O'Malley, "Performance enhancement of a haptic arm exoskeleton," in *Haptic Interfaces for Virtual Environment and Teleoperator Systems, 2006 14th Symposium on,* 2006, pp. 375-381.

[8] A. Gupta and M. K. O'Malley, "Design of a haptic arm exoskeleton for training and rehabilitation," in *Mechatronics, IEEE/ASME Transactions on,* 2006, pp. 280-289.

[9] R. J. Sanchez, E. T. Wolbrecht, R. Smith, J. Liu, S. Rao, S. Cramer, T. Rahman, J. E. Bobrow and D. J. Reinkensmeyer, "A pneumatic robot for re-training arm movement after stroke: Rationale and mechanical design," in *Rehabilitation Robotics, 2005. ICORR 2005. 9th International Conference on,* 2005, pp. 500-504.

[10] R. J. Sanchez, J. Liu, S. Rao, P. Shah, R. Smith, T. Rahman, S. C. Cramer, J. E. Bobrow and D. J. Reinkensmeyer, "Automating arm movement training following severe stroke: Functional exercises with quantitative feedback in a gravity-reduced environment," in *Neural Systems and Rehabilitation Engineering, IEEE Transactions on [See also IEEE Trans. on Rehabilitation Engineering],* 2006, pp. 378-389.

[11] M. Mihelj, T. Nef and R. Riener, "ARMin II - 7 DoF rehabilitation robot: Mechanics and kinematics," in *Robotics and Automation, 2007 IEEE International Conference on,* 2007, pp. 4120-4125.

[12] A. Jackson, P. Culmer, S. Makower, M. Levesley, R. Richardson, A. Cozens, M. M. Williams and B. Bhakta, "Initial patient testing of iPAM - a robotic system for stroke rehabilitation," in *Rehabilitation Robotics, 2007. ICORR 2007. IEEE 10th International Conference on,* 2007, pp. 250-256.

[13] G. Rosati, P. Gallina and S. Masiero, "Design, implementation and clinical tests of a wire-based robot for neurorehabilitation," in *Neural Systems and Rehabilitation Engineering, IEEE Transactions on [See also IEEE Trans. on Rehabilitation Engineering],* 2007, pp. 560-569.

[14] A. Mayr, M. Kofler and L. Saltuari, "An electromechanical robot for upper limb training following stroke. A prospective randomised controlled pilot study," *Handchirurgie Mikrochirurgie Plastische Chirurgie*, vol. 40, pp. 66-73, FEB 2008.

[15] N. Hogan, H. Krebs, A. Sharon and J. Charnnarong, "Interactive Robot Therapist," 5466213, November 14, 1995, 1995.

[16] D. J. Reinkensmeyer, L. E. Kahn, M. Averbuch, A. McKenna-Cole, B. D. Schmit and W. Z. Rymer, "Understanding and treating arm movement impairment after chronic brain injury: progress with the ARM guide," J. *Rehabil. Res. Dev.*, vol. 37, pp. 653-662, 11. 2000.

[17] S. Coote, E.K. Stokes, B.T. Murphy and W.S. Harwin "The effect of GENTLE/s robot mediated therapy on upper extremity function post

stroke" *Proceedings International Conference on Rehabilitation Robotics Korea* pp. 59-61 (April 22-25 2003)
[18] S. Hesse, C. Werner, M. Pohl, S. Rueckriem, J. Mehrholz and M. L. Lingnau, "Computerized Arm Training Improves the Motor Control of the Severely Affected Arm After Stroke: A Single-Blinded Randomized Trial in Two Centers," *Stroke*, vol. 36, pp. 1960-1966, September 1. 2005.
[19] R. Riener, T. Nef and G. Colombo, "Robot-aided neurorehabilitation of the upper extremities," *Med. Biol. Eng. Comput.*, vol. 43, pp. 2-10, 01. 2005.
[20] R. A. Schmidt and T. D. Lee, *Motor Control and Learning: A Behavioral Emphasis*. ,3rd Edition ed.Champaign, Illinois: Human Kinetics Publishers, 1998, pp. 495.
[21] P. S. Lum, C. G. Burgar, Van der Loos, M., P. C. Shor, M. Majmundar and R. Yap, "The MIME robotic system for upper-limb neuro-rehabilitation: Results from a clinical trial in subacute stroke," in *Rehabilitation Robotics, 2005. ICORR 2005. 9th International Conference on, 2005*, pp. 511-514.
[22] A. Toth, G. Fazekas, G. Arz, M. Jurak and M. Horvath, "Passive robotic movement therapy of the spastic hemiparetic arm with REHAROB: Report of the first clinical test and the follow-up system improvement," in *Rehabilitation Robotics, 2005. ICORR 2005. 9th International Conference on*, 2005, pp. 127-130.
[23] Y. Hurmuzlu, A. Ephanov and D. Stoianovici, "Effect of a Pneumatically Driven Haptic Interface on the Perceptional Capabilities of Human Operators," Presence: Teleoperators & Virtual Environments, vol. 7, pp. 290-307, 06/15. 1998.
[24] M. Bergamasco, B. Allotta, L. Bosio, L. Ferretti, G. Parrini, G. M. Prisco, F. Salsedo and G. Sartini, "An arm exoskeleton system for teleoperation and virtual environments applications," in *Robotics and Automation, 1994. Proceedings., 1994 IEEE International Conference on,* 1994, pp. 1449-1454 vol.2.
[25] A. Frisoli, F. Rocchi, S. Marcheschi, A. Dettori, F. Salsedo and M. Bergamasco, "A new force-feedback arm exoskeleton for haptic interaction in virtual environments," in *Eurohaptics Conference, 2005 and Symposium on Haptic Interfaces for Virtual Environment and Teleoperator Systems, 2005. World Haptics 2005. First Joint,* 2005, pp. 195-201.
[26] T. G. Sugar, Jiping He, E. J. Koeneman, J. B. Koeneman, R. Herman, H. Huang, R. S. Schultz, D. E. Herring, J. Wanberg, S. Balasubramanian, P. Swenson and J. A. Ward, "Design and control of RUPERT: A device for robotic upper extremity repetitive therapy," in *Neural Systems and Rehabilitation Engineering, IEEE Transactions on [See also IEEE Trans. on Rehabilitation Engineering],* 2007, pp. 336-346.
[27] C. Carignan, M. Liszka and S. Roderick, "Design of an arm exoskeleton with scapula motion for shoulder rehabilitation," in *Advanced Robotics, 2005. ICAR '05. Proceedings., 12th International Conference on,* 2005, pp. 524-531.
[28] M. Bergamasco, B. Allotta, L. Bosio, L. Ferretti, G. Parrini, G. M. Prisco, F. Salsedo and G. Sartini, "An arm exoskeleton system for teleoperation and virtual environments applications," in *Robotics and Automation, 1994. Proceedings., 1994 IEEE International Conference on*, 1994, pp. 1449-1454 vol.2.
[29] A. Schiele and van der Helm, F.C.T., "Kinematic design to improve ergonomics in human machine interaction," in *Neural Systems and Rehabilitation Engineering, IEEE Transactions on [See also IEEE Trans. on Rehabilitation Engineering],* 2006, pp. 456-469.
[30] L. Q. Zhang, H. S. Park and Y. Ren, "Developing an intelligent robotic arm for stroke rehabilitation," in *Rehabilitation Robotics, 2007. ICORR 2007. IEEE 10th International Conference on*, 2007, pp. 984-993.
[31] M. Mihelj, T. Nef and R. Riener, "ARMin - toward a six DoF upper limb rehabilitation robot," in *Biomedical Robotics and Biomechatronics, 2006. BioRob 2006. the First IEEE/RAS-EMBS International Conference on,* 2006, pp. 1154-1159.
[32] B. D. Adelstein, "Three degree of freedom parallel mechanical linkage," USA 5816105, Oct 6, 1998, 1998.
[33] J. L. Emken, J. E. Bobrow and D. J. Reinkensmeyer, "Robotic movement training as an optimization problem: Designing a controller that assists only as needed," in *Rehabilitation Robotics, 2005. ICORR 2005. 9th International Conference on,* 2005, pp. 307-312.
[34] C. D. Takahashi, L. Der-Yeghiaian, V. H. Le and S. C. Cramer, "A robotic device for hand motor therapy after stroke," in *Rehabilitation Robotics, 2005. ICORR 2005. 9th International Conference on*, 2005, pp. 17-20.
[35] E. T. Wolbrecht, J. Leavitt, D. J. Reinkensmeyer and J. E. Bobrow, "Control of a pneumatic orthosis for upper extremity stroke rehabilitation," in *Engineering in Medicine and Biology Society, 2006. EMBS '06. 28th Annual International Conference of the IEEE,* 2006, pp. 2687-2693.
[36] T. Rahman, W. Sample and R. Seliktar, "Design and testing of WREX," *The Eighth International Conference on Rehabilitation Robotics*, Kaist, Korea, 2003.
[37] M. V. Radomski and C. T. Trombly Latham, Occupational Therapy for Physical Dysfunction. ,6th ed.Philadelphia: Lippincott Williams & Wilkins, 2008, pp. 1432.
[38] A. Kecskeméthy and A. Weinberg, "An Improved Elasto-Kinematic Model of the Human Forearm for Biofidelic Medical Diagnosis," *Multibody System Dynamics,* vol. 14, pp. 1-21, 2005.
[39] J. C. Perry, J. Rosen and S. Burns, "Upper-limb powered exoskeleton design," in *Mechatronics, IEEE/ASME Transactions on*, 2007, pp. 408-417.
[40] M. Šenk and L. Chèze, "Rotation sequence as an important factor in shoulder kinematics," *Clinical Biomechanics,* vol. 21, pp. S3-S8, 2006
[41] G. Wu, van der Helm,Frans C.T., H. E. J. (DirkJan) Veeger, M. Makhsous, P. Van Roy, C. Anglin, J. Nagels, A. R. Karduna, K. McQuade, X. Wang, F. W. Werner and B. Buchholz, "ISB recommendation on definitions of joint coordinate systems of various joints for the reporting of human joint motion—Part II: shoulder, elbow, wrist and hand," *Journal of Biomechanics,* vol. 38, pp. 981-992, 5. 2005.
[42] J.M. McCarthy, *Geometric Design of Linkages (Interdisciplinary Applied Mathematics)*. Springer, 2000, pp. 320.
[43] R. Murray, Z. Li and S. Sastry, *A Mathematical Introduction to Robotic Manipulation*. Boca Raton, FL.: CRC Press, 1994, pp. 456.
[44] T. Kang, J. He and S. I. Tillery, "Determining natural arm configuration along a reaching trajectory," *Experimental Brain Research*, vol. 167, pp. 352-361, October 20, 2005.
[45] J. P. A. Dewald and R. F. Beer, "Abnormal joint torque patterns in the paretic upper limb of subjects with hemiparesis," *Muscle & Nerve*, vol. 24, pp. 273-283, 2001.
[46] A. R. Fugl-Meyer, L. Jääskö, I. Leyman, S. Olsson and S. Steglind, "The post-stroke hemiplegic patient. 1. A method for evaluation of physical performance," *Scand J Rehabil Med.*, vol. 7, pp. 13-31, 1975.
[47] NASA. (2005, 6/15/05). Man-systems integration standards revision B - NASA-STD-3000. *MSIS 2008 (4/20/08)*, Available: msis.jsc.nasa.gov

Julius Klein received a B.S. degree in industrial engineering from Universitat de Girona, Catalunya, Spain in 2003, and an M.S. degree in mechanical and aerospace engineering from the University of California, Irvine, in 2005. He is currently a PhD candidate in the Department of Mechanical and Aerospace Engineering at the University of California, Irvine. Mr. Klein's research interests include robotics, nonlinear control, fabrication processes, motor learning, and neurorehabilitation.